

Structural and Thermal Behavior of Comb-Like Polymer Having *n*-Octadecyl Side Chains

Prakash J. Saikia, Shashi D. Baruah

Regional Research Laboratory, Jorhat 785 006, Assam, India

Received 1 December 2005; accepted 3 November 2006

DOI 10.1002/app.25773

Published online in Wiley InterScience (www.interscience.wiley.com).

ABSTRACT: The cocrystallization behavior of poly(*n*-octadecyl methacrylate) (POMA) and its blends with corresponding fatty acid (*n*-octadecanoic acid) (C₁₈) was explored by differential scanning calorimetry (DSC) and X-ray diffraction studies. The DSC curves for blended samples of POMA with C₁₈ show the characteristic melting endotherms that correspond to the melting of the crystallites. The existence of hexagonally packed crystalline lattice is confirmed

from the X-ray diffraction studies. Thermal degradation of the polymer and its blend proceeds in a one-step reaction. © 2007 Wiley Periodicals, Inc. *J Appl Polym Sci* 104: 1226–1231, 2007

Key words: poly(*n*-octadecyl methacrylate); comb-like polymers; cocrystallization; differential scanning calorimetry; X-ray diffraction; thermal degradation

INTRODUCTION

Macromolecules with *n*-alkyl side chains are denoted as comb-like polymers and have been intensively studied in recent years owing to their intermediate place between linear and branched polymers.¹ Comb-like polymers with pendent alkyl side chains of specific length have been extensively used as flow improvers (FIs) or pour point depressants (PPD) for transportation of waxy crude oils. These chemicals reduce the pour point (lowest temperature at which the oil flows), viscosity, and yield stress of the crude oils considerably, enabling the transportation of the crude oils well below the natural pour points. The FIs or PPDs resemble the *n*-alkane, which comprises the bulk of the wax. These additives modify the wax crystal structure either by cocrystallization or by adsorption, producing smaller crystals of higher volume to surface area ratio, thus preventing gelation.² These comb-like polymers adsorb strongly to the main growth faces of the wax crystal, and do so in a manner that breaks down the characteristic lamellar structure found in wax crystal.³ These polymers crystallize through alkyl side chain packing, independently of the stereoregularity of the main chain. Comb-like polymers, which have crystallizable poly(*n*-alkyl) side chains being attached to the amorphous main chain, are known to pack into layered structure with alternating crystalline side chain region and amorphous main chain region in the solid state.⁴ Poly(*n*-octadecyl methacrylate) (POMA) may be considered a typical

short branched comb-like polymer because each molecule has one long alkyl side chain on every two main chain carbon atoms. X-ray diffraction (XRD) profile of such polymers has an intense reflection corresponding to the Bragg spacing *d* of 4.16 Å, which suggests formation of hexagonal crystalline lattice of *n*-alkyl side chain.⁵ There also exists a shoulder in smaller angle region that is considered to originate from layered structure. To establish the diffraction pattern of POMA and poly(*n*-octadecyl acrylate) (POA), Plate and Shibalev⁶ proposed a two-layered structure for POMA and a one-layered structure for POA. In the former model, the side chains extended on both sides of the main chain. In the latter structure, disordered packing of the end groups of the side chains occur and the polymer chains are arranged with the shift towards the extended side chain axis, which leads to smaller value of layer spacing. On the basis of the intensity distribution of X-ray reflection in small angle region, Hsieh et al.⁷ reported that the intercalating side chains pointing in opposite direction form the crystalline layer. Although detailed solid-state structure of comb-like polymers has not been established, the layered structure with alternating segregation of the side chain and main chain domain is commonly accepted.⁸ The crystallization behavior of linear alkanes with 10–25 carbons has also been studied in detail.⁹ Somehow the crystallization of long alkyl groups in side chain polymers might be seen as a crystallization of alkanes in the presence of external constrains. The crystallization behavior of long alkyl groups in side chain polymers has been studied by different techniques^{10–14} and it is known that the alkyl groups in the substance can crystallize at room temperature. Otherwise, the constrains by the methacrylate backbone are still remarkable so that only one-

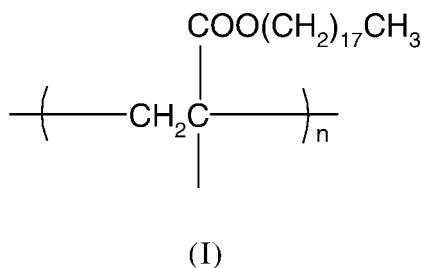
Correspondence to: S. D. Baruah (baruah_shashi@yahoo.co.in).

third of the CH₂ units in the alkyl group can crystallize easily.¹⁵

n-Octadecanoic acid has a chemical structure similar to that of the side chain of the polymer and crystallizes at a temperature higher than the crystallization temperature of POMA. DSC studies of the polymers indicated that their alkyl side chains could crystallize in the same order as that of the neat polymer. The aim of the present work is to study whether the C₁₈ side chains of POMA would cocrystallize with the C₁₈ side chains of the *n*-octadecanoic acid. The dependence of long *n*-alkyl side chains of POMA on thermal degradation is also presented in the article. The XRD profile of the blends shows cocrystallization behavior.

EXPERIMENTAL

Poly(*n*-octadecyl methacrylate) (POMA, I) with low polydispersity was prepared by atom transfer radical polymerization (ATRP) as described in a previous paper.⁵ The polymer was purified by repeated precipitation in acetone. The number-average molecular weight (*M_n*) of the sample was 6600, with a polydispersity index of 1.51. *n*-Octadecanoic acid (CH₃(CH₂)₁₆-COOH, C₁₈, Merck) and tetrahydrofuran (THF; Qualigens, India) were purified by standard methods.



The blending samples of POMA with C₁₈ were prepared as follows: The weighted polymer and C₁₈ were refluxed in THF at 80°C, quenched to room temperature, and dried in vacuum at 30°C for 48 h till a constant weight is obtained. Blended samples were grounded to a fine powder to prepare homogeneously mixed samples. The compositions of the blends are expressed by the mole fraction of the monomeric units of polymer and C₁₈. Molecular weights (MWs) and molecular weight distribution (MWD) of the polymers were determined using a Waters 515 gel permeation chromatograph equipped with three styragel columns (HR1, HR3, and HR4) in series with a 2410 differential refractometer as the detector. The analysis was performed at room temperature with purified high-performance liquid chromatography grade THF as eluent at 1.0 mL min⁻¹. Calibration was based on narrow MWD polystyrene standards with the Waters Millennium 2.0 software package. DSC curves were recorded using a TA series DSC 2010 instrument

under nitrogen atmosphere with 2–5 mg of polymer samples weighed in aluminum pan at a heating rate of 10°C min⁻¹. The instrument was calibrated with indium for correction of heat of transition. Thermal stability studies were performed using a TA series STD 2960 simultaneous DTA-TGA analyzer under nitrogen atmosphere with 10–15 mg of polymer samples at a heating rate of 10°C min⁻¹. DSC and DTA-TGA runs were repeated thrice for each sample. The X-ray diffractograms of polymer samples were recorded on a model JDX-11P3A JEOL diffractometer with a solid sample using Ni filtered Cu-Kα radiation at 35 kV and 10 mA in the wide angle range 2° < θ < 60°. The samples for obtaining X-ray diffractograms were presented in film form with a sample size of 7–10 mg.

RESULTS AND DISCUSSION

In the solid-state of POMA blended with *n*-dodecane and *n*-octadecane, side chains of the polymers were found to cocrystallize with *n*-hydrocarbon and to alter the solid-state structure of low MW component.¹⁶ This suggests that cocrystallization is produced because of the thermodynamically miscible parts of two components in the blend having similar crystallization rates.^{17,18} The main chain of POMA strongly influences the crystallization behavior of *n*-octadecyl side chain.¹⁹ So it is interesting to study whether the side chains of polar *n*-octadecanoic acid cocrystallize with the nonpolar C₁₈ side chains of the POMA homopolymers. To investigate the cocrystallization behavior of POMA with the corresponding fatty acid (C₁₈), the DSC curves of the blended samples of POMA with C₁₈ were recorded under nitrogen atmosphere at a heating rate of 10°C min⁻¹ (Fig. 1). The characteristic melting endotherms corresponding to the melting of the crystallites are evident in almost all

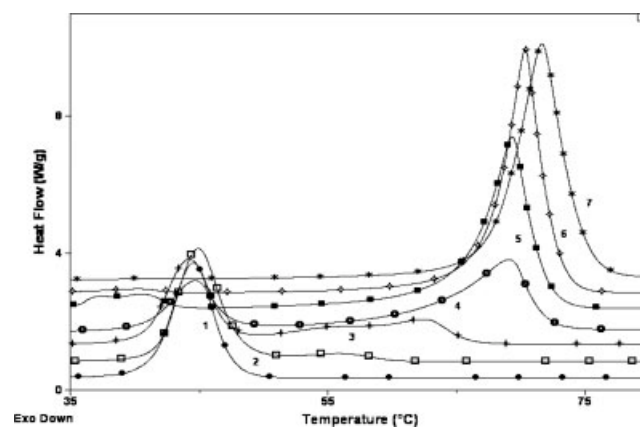


Figure 1 DSC curves for POMA blends with C₁₈, recorded under nitrogen atmosphere at a heating rate of 10°C min⁻¹. Mole percent of [POMA]/[C₁₈] = (●), 100/0; (□), 90/10; (+), 75/25; (○), 50/50; (■), 25/75; (◇), 10/90; (*), 0/100.

TABLE I
Differential Scanning Calorimetric Studies of POMA Blended with *n*-Octadecanoic Acid (C₁₈)

Sample no.	POMA (mol %)	C ₁₈ (mol %)	First transition			Second transition		
			Peak value (°C)	ΔH_m (kJ mol ⁻¹)	ΔS_m (J K ⁻¹ mol ⁻¹)	Peak value (°C)	ΔH_m (kJ mol ⁻¹)	ΔS_m (J K ⁻¹ mol ⁻¹)
1	100	0	44.5	28.51	89.79	–	–	–
2	90	10	44.8	27.57	86.74	56.9	1.09	3.30
3	75	25	44.1	20.02	63.13	62.6	10.22	30.47
4	50	50	44.7	13.96	43.94	69.1	27.87	81.50
5	25	75	40.7	3.75	11.94	69.4	49.87	145.68
6	10	90	39.6	2.02	6.47	70.3	57.25	166.76
7	0	100	–	–	–	71.6	66.70	193.54

POMA, poly(*n*-octadecyl methacrylate).

samples. The melting points (mp) and the heats of fusion (ΔH_m) were determined from the endothermic peaks. The entropy of fusion (ΔS_m) is calculated from the mp and ΔH_m values. The relationship between the thermodynamic parameters of fusion (mp, ΔH_m , and ΔS_m) and molar ratios of POMA with C₁₈ is illustrated in Table I. ΔS_m values were calculated from T and ΔH_m values assuming that ΔG_m is zero. At $\Delta G_m = 0$, in the reaction the products and reactants are equally favored. For the first transition, the ΔH_m and ΔS_m decrease with the increase in C₁₈ content and for the second transition an increase in the corresponding values are observed with the increase in C₁₈ (Fig. 1). This gives C₁₈ an advantage to crystallize even at content as low as 10%. The crystallization of POMA may be inhibited by the restricted mobility of the POMA chains and could remain as amorphous without crystallizing. However, with the increase of mole percent of POMA, the crystallization starts. The melting endotherms show individual melting peaks for POMA and C₁₈. For pure POMA an endothermic peak occurred at 44.5°C. With 25 mol % of C₁₈ content, another endothermic peak is observed at higher temperature region. With the increase of C₁₈ content, the position of the peak moved towards the pure C₁₈ (71.6°C). Shapes and temperatures of the transition peaks vary with the change in C₁₈ content. Its height and temperature increase with C₁₈ content and temperature approaches the crystallization point of pure C₁₈. The crystallization temperature against mole fraction of C₁₈ content indicates the formation of a new crystalline form at 25 mol %, and eutectic crystallization of the new crystalline form with the crystallite of POMA occurs in the range of 0–25% (Fig. 1). Another eutectic crystallization⁸ (simultaneous crystallization of the constituents of a eutectic mixture during cooling of the melt) of a new form with the crystalline C₁₈ occurs in the range of 25–100 mol %. From the DSC thermogram, the plot of heat of crystallization for 1 mol of octadecyl side chain, ΔH_{side} , suggests that the added C₁₈ content influences the crystallization behavior of the side chain (Fig. 2). The

increase in ΔH_{side} with C₁₈ content indicates the increase in number of methylene units in the hexagonally packed crystalline domain. This indicates that the blended C₁₈ molecules are incorporated into the crystalline lattice formed by the side chains of polymer.⁴ So, it is proved that C₁₈ molecules in the solid state are cocrystallizing with *n*-octadecyl side chains. The above-mentioned interpretation for the phase behavior is in conformity with the X-ray profile of the blended samples.

Although the coexistence of the ordered and disordered arrangements of end-to-end form is not clearly confirmed because the peak for the C₁₈ content is diffuse, the DSC curves for more than 25 mol % of C₁₈ suggest the coexistence of end-to-end form.⁸ These results of DSC measurements confirm the transformation of the layered structure. For the state of crystalline domain containing both *n*-octadecyl side chain and C₁₈, the heat of crystallization for 1 mol of *n*-alkyl

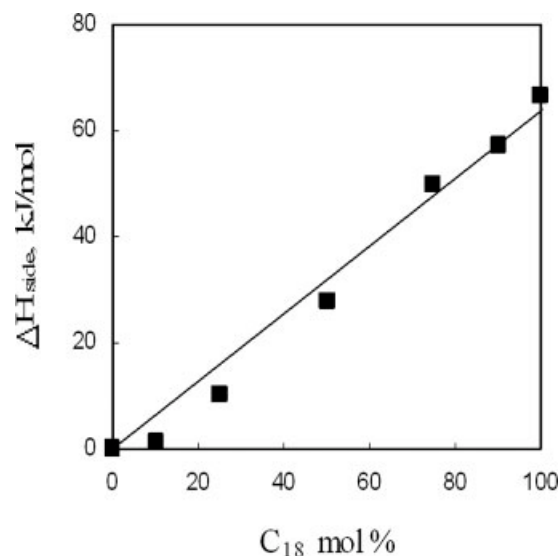


Figure 2 Plot of heat of crystallization per mole of *n*-octadecyl side chain, ΔH_{side} , versus C₁₈ content in blends of POMA/C₁₈.

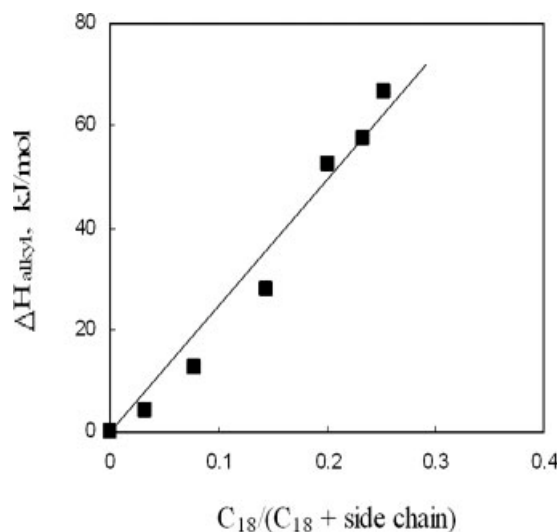


Figure 3 Plot of ΔH_{alkyl} versus fraction of C_{18} content in all n -alkyl chains ($= C_{18}/(C_{18} + \text{side chain})$).

chain, ΔH_{alkyl} (n -octadecyl side chain and C_{18} molecule), is calculated. Figure 3 shows the plot of ΔH_{alkyl} against the fraction of C_{18} in the total n -alkyl chain ($C_{18}/(C_{18} + \text{side chains})$). From the figure it is prominent that ΔH_{alkyl} increases with increasing C_{18} content for POMA and its blended sample. For one n -alkyl chain, the cocrystallization behavior of comb-like polymer with C_{18} increases the average number of methylene units that existed in the hexagonally packed crystalline domain.⁴

X-ray diffraction measurements of POMA and different blends of POMA with C_{18} are carried out at room temperature. The diffraction pattern of POMA shows a peak at about $2\theta = 21.6^\circ$, which corresponds to an interplanar distance of 4.12\AA . This value is in agreement with the value of several long chain acrylate and methacrylate comb-like polymers, attributed to the van der Waal's contraction of nonbonded atom.⁸ The spacing at 4.12\AA corresponds to the typical hexagonally packed cylinders of n -alkane crystals close to their mp's. This peak may be originated from the disordering in the alkyl segments or the amorphous phase. Besides this peak, a very sharp peak at a very low angle (3°) is apparent (Fig. 4). These peaks may be assigned to the layered structure of the alternating crystalline side chain region and amorphous region. In the diffraction pattern of blends with 25 mol % of C_{18} content or less, only these two peaks with varied intensities are observed. With more than 25 mol % of C_{18} , an additional peak appeared at $2\theta = 24.1^\circ$ and the intensity of the peak increases with the increase in C_{18} content (Fig. 4). Therefore, blends containing more than 25 mol % of C_{18} , the separated C_{18} crystallites, are coexisting with the hexagonal crystalline lattice and the newly appeared peaks can be assigned to the crystallite in C-form of C_{18} .⁸ The

alkyl chains of both POMA and C_{18} are packed together to form the stereochemically acceptable sub cell structure. In the samples containing less than 25 mol % of C_{18} , the absence of XRD peaks and DSC transition corresponding to the pure C_{18} confirms the existence of only hexagonally packed crystalline lattice. From the XRD patterns of the blends containing more than 25 mol % C_{18} , it can be observed that the isolated C_{18} crystallites coexist in the hexagonal crystalline lattice. Poly(n -alkyl) acrylates and methacrylates crystallize in hexagonal packing (in accordance with X-ray studies) as characterized by a single absorption band¹ at 720 cm^{-1} . POMA used in the present system also shows a single absorption band at 722 cm^{-1} , indicating that the long alkyl side chains of POMA are of the hexagonal type packing.¹²

The primary method for monitoring pyrolysis of polymers is thermogravimetric analysis (TGA). TGA is used to determine chemical structure and the pyrolytic properties of polymers by measuring the mass volatilized as a function of time. Although the chemical reactions underlying the pyrolysis are known, the usual methods for interpreting TGA data are based on distribution kinetics, a comprehensive approach for dynamics of systems having a distributed property.²⁰ The model describes the isothermal and constant heating rate TGA as a function of time and temperature. Thermal degradation of POMA and its blended samples with C_{18} proceeded via a one-step reaction, i.e., $T_{\text{ini}} = 150\text{--}200^\circ\text{C}$ and $T_{\text{max}} = 325\text{--}400^\circ\text{C}$. In the comb-like polymers with bulky n -alkyl group,

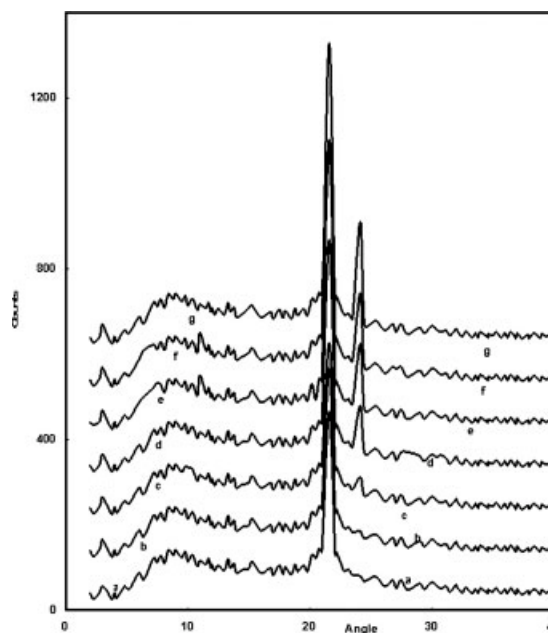


Figure 4 X-ray diffraction patterns of for POMA blends with C_{18} , measured at room temperature. Mole percent of $[POMA]/[C_{18}] =$ (a) 100/0; (b) 90/10; (c) 75/25; (d) 50/50; (e) 25/75; (f) 10/90; (g) 0/100.

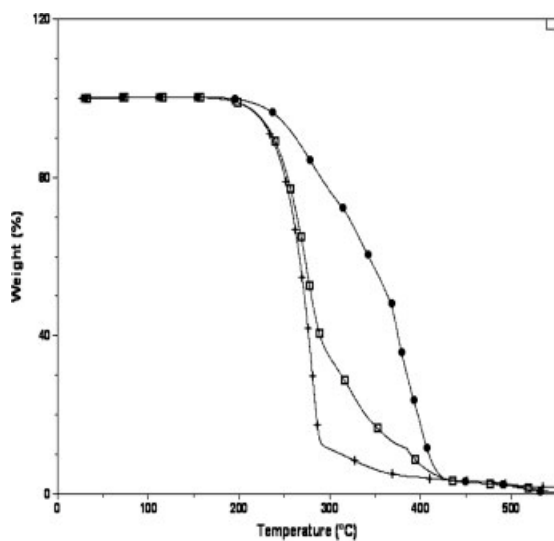


Figure 5 Thermogravimetric analysis of POMA blends with C_{18} , recorded under nitrogen atmosphere at a heating rate of $10^{\circ}\text{C min}^{-1}$. Mole percent of $[\text{POMA}]/[C_{18}] = (\bullet)$, 100/0; (\square) , 50/50; $(+)$, 10/90.

the weight residue at 500°C was below 2%, suggesting that depolymerization to OMA monomer occurs similar to poly(methyl methacrylate). The results of TGA of neat POMA and its blends with 50 and 90 mol % of C_{18} are shown in Figure 5. Kinetic parameters for neat POMA and its blends with 50 and 90 mol % of C_{18} are calculated from nonisothermal TG curves using nonmechanistic equations of Freeman and Carroll²¹ (Fig. 6) and Flynn and Wall²² (Fig. 7) and the results are found to be in good agreement with each other.

The Freeman and Carroll equation²¹

The final equation derived from the modified treatment of the Freeman and Carroll method can be represented in the differential form as

$$\log[Q(dW/dT)/W_r] = -E/2.303RT + \log A$$

where, $W_r = W_o - W_t$, W_o is the total mass loss in the decomposition process, W_t is the total weight loss at any time t , Q is the constant heating rate, which is $10^{\circ}\text{C min}^{-1}$ (4.66 K min^{-1}), A is the Arrhenius preexponential factor, R is the universal gas constant, and E is the activation energy.

The Flynn and Wall equation²²

The simplified differential rate expression and weight-loss-time equation of the Flynn and Wall can be represented in the form of

$$\log[(dw/dT)/(W_o - W_t)^n] = -E/2.303RT + \log A$$

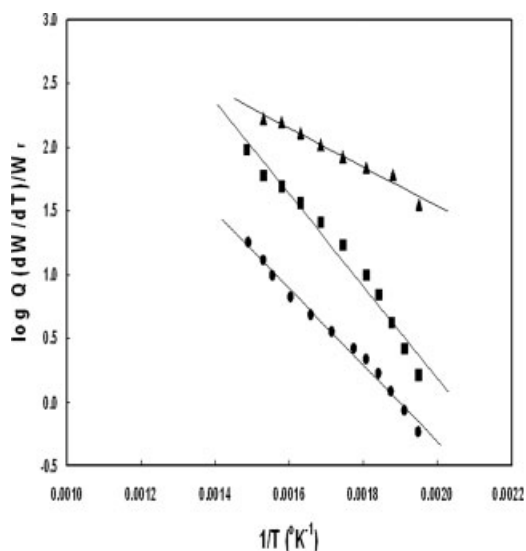


Figure 6 Freeman and Carroll plot for POMA blends with C_{18} . Mole percent of $[\text{POMA}]/[C_{18}] = (\blacktriangle)$, 10/90; (\blacksquare) , 50/50; (\bullet) , 100/0.

where the terms have the same meaning as those of the Freeman and Carroll equation. Curves can be drawn for different values of n in the range of 0–2 and E was fixed from the value of n , which gave the best-fit line. For both the equations, the slope of the plot of left hand side of the equation versus $1/T$ is $-E/2.303R$ from which E can be calculated (Figs. 6 and 7). Table II shows the activation energies and the values of correlation coefficient r obtained by two different methods employed in this work. The average activation energies for POMA and its blends with 50 and 90 mol % of C_{18} are found to be 59.65, 69.14, and 28.59 kJ mol^{-1} , respectively. These results show that

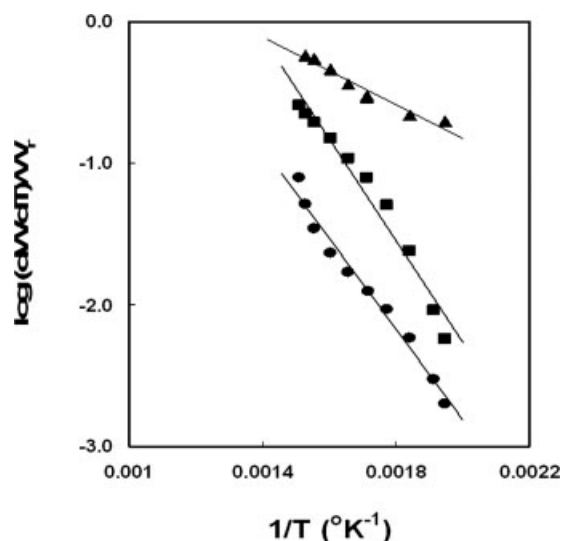


Figure 7 Flynn and Wall plot for POMA blends with C_{18} . Mole percent of $[\text{POMA}]/[C_{18}] = (\blacktriangle)$, 10/90; (\blacksquare) , 50/50; (\bullet) , 100/0.

TABLE II
Thermal Decomposition Temperatures, Activation Energies (E), and Correlation Coefficients (r) of POMA Blended with n -Octadecanoic Acid (C_{18})

Sample		Temperature range ($^{\circ}C$)	Freeman and Carroll method		Flynn and Wall method	
POMA (mol %)	C_{18} (mol %)		E ($kJ\ mol^{-1}$)	r	E ($kJ\ mol^{-1}$)	r
100	0	230.0–390.0	57.47	0.99	61.83	0.98
50	50	230.0–390.0	69.39	0.97	68.89	0.97
10	90	230.0–390.0	29.43	0.98	27.74	0.95

POMA, poly(n -octadecyl methacrylate).

the thermal stabilities of POMA and POMA- C_{18} blends are described by the stability of polymer backbones to the random main chain scission and do not depend on the stability of the side chains. Further experiments in more detail seem to be required to prove the assumption. A meaningful analysis of the variation in activation energies would require development of a detailed kinetic model of the decomposition process, including detailed kinetic models of all elementary reaction steps, which is beyond the scope of this article.

CONCLUSIONS

Cocrystallization behavior of comb-like polymers with long alkyl groups has been extensively studied but still not much is known about the details of the side chain crystallization process in these systems. Cocrystallization behavior of POMA with C_{18} shows the characteristic melting endotherms of the crystallites. This suggests that the addition of C_{18} induces the crystallization of the side chain for the amorphous comb-like polymers. Eutectic crystallization⁸ of the new crystalline forms with the POMA crystallites occurred in different ranges and was evident by the X-ray profile of the blended samples. In general, the presented results indicate the cocrystallization behavior of POMA with C_{18} and the transition of alkyl group from the amorphous to crystalline state. X-ray diffraction and thermal studies have contributed to a better understanding of the overall blend structure of POMA with C_{18} . The morphology of blends is dependent on the crystallization condition. Some features of the side chain crystallization in POMA/ C_{18} system resemble effects observed for other systems with long CH_2 sequences like alkanes and polyethylene.

The authors thank Dr. P.G. Rao, Director, Regional Research Laboratory, Jorhat, for permission to publish the results.

References

1. Yokota, K.; Kougo, T.; Hirabayashi, T. *Polym J* 1983, 12, 891.
2. Wardhaugh, L. T.; Boger, D. V. *AIChE J* 1991, 36, 871.
3. Duffy, D. M.; Rodger, P. M. *Phys Chem Chem Phys* 2002, 4, 328.
4. Inomata, K.; Sakamaki, Y.; Nose, T.; Sasaki, S. *Polym J* 1996, 28, 986.
5. Saikia, P. J.; Dass, N. N.; Baruah, S. D. *J Appl Polym Sci* 2005, 97, 2140.
6. Plate, N. A.; Shibaev, V. P. *J Polym Sci Part D: Macromol Rev* 1974, 8, 117.
7. Hsieh, H. W. S.; Post, B.; Morawetz, H. J. *J Polym Sci Polym Phys Ed* 1976, 14, 1241.
8. Inomata, K.; Sakamaki, Y.; Nose, T.; Sasaki, S. *Polym J* 1996, 28, 992.
9. Montenegro, R.; Antonietti, M.; Matsai, Y.; Landfester, K. *J Phys Chem* 2003, B107, 5088.
10. Pitsikalis, M.; Siakali-Kioulafa, E.; Hadjichristidis, N. *Macromolecules* 2000, 33, 5460.
11. Alig, I.; Jarek, M.; Hellmann, G. P. *Macromolecules* 1998, 31, 2245.
12. Kunisada, H.; Yuki, Y.; Kondo, S. *Macromolecules* 1991, 24, 4733.
13. Coskun, M.; Temüz, M. M.; Koca, M. *Polym Degrad Stab* 2003, 81, 95.
14. Hempel, E.; Huth, H.; Beiner, M. *Thermochim Acta* 2003, 403, 105.
15. Hempel, E.; Budde, H.; Horing, S.; Beiner, M. *J Non-Cryst Solids* 2006, 352, 5013.
16. Rubin, I. D.; Pugliese, R. D. *Angew Makromol Chem* 1989, 171, 156.
17. Xu, J.; Xu, X.; Chen, L.; Feng, L.; Chen, W. *Polymer* 2001, 42, 3867.
18. Hennessy, A.; Neville, A.; Roberts, K. *J Crystal Growth Design* 2004, 4, 1069.
19. Jordan, E. F., Jr.; Artymyshyn, B.; Specca, A.; Wrigley, A. N. *J Polym Sci Part A-1: Polym Chem* 1971, 9, 3349.
20. Kodaera, Y.; McCoy, B. *J Energy Fuels* 2002, 16, 119.
21. Freeman, E. S.; Carroll, B. *J Phys Chem* 1958, 62, 394.
22. Flynn, J. H.; Wall, L. A. *J Res Natl Bur Stand Sect A* 1966, 70, 487.